Performance Analysis of a Class of Nondata-Aided Frequency Offset and Symbol Timing Estimators for Flat-Fading Channels

Yan Wang, Philippe Ciblat, Erchin Serpedin, and Philippe Loubaton, *Member, IEEE*

***Abstract*—Nondata-aided carrier frequency offset and symbol timing delay estimators for linearly modulated waveforms transmitted through flat-fading channels have been recently developed by exploiting the received signal's second-order cyclostationary statistics. The goal of this paper is to establish and analyze the asymptotic (large sample) performance of the estimators as a function of the pulse shape bandwidth and the oversampling factor. It is shown that selecting larger values for the oversampling factor does not improve the performance of these estimators, and the accuracy of symbol timing delay estimators improves as the pulse shape bandwidth increases.**

***Index Terms*—Cyclic correlation, cyclostationarity, fractionally sampling, synchronization.**

I. Introduction

In MOBILE radio channels, loss of synchronization often occurs, and reacquisition must be performed in a fast and reliable way without sacrificing bandwidth for periodic retraining. Therefore, developing improved performance nondata-aided (or blind) synchronization architectures appears to be an important problem. Recently, blind carrier frequency offset and symbol timing delay estimators that exploit the second-order cyclostationary statistics, which have been introduced by oversampling or fractionally sampling the continuous-time received waveform at a rate faster than Nyquist rate, have been proposed in [6], [7], and [14].

The goal of this paper is to analyze the performance of the feedforward nondata-aided carrier frequency offset and symbol timing delay estimators [6], [7] with respect to (w.r.t.) the pulse shape bandwidth and the oversampling factor. The theoretical asymptotic (large sample) performance of the Gini–Giannakis (GG) [7] and Ghogho–Swami–Durrani (GSD) [6] estimators is established, and it is shown that the performance of these estimators does not improve by selecting a large value for the oversampling factor ($P > 3$) and that the accuracy of the timing delay estimators can increase by choosing pulse shapes with larger bandwidths. By properly taking into account the aliasing effects, it is shown that the expressions of the symbol timing delay estimators take a slightly different form than the expressions reported in [6] and [7] when $P = 2$.

The rest of this paper is organized as follows. In Section II, the discrete-time channel model is established, and the necessary modeling assumptions are invoked. Section III briefly introduces the GG and GSD estimators, whose asymptotic performance analysis for time-invariant channels is established in Section IV. The results of Section IV are extended to time-selective fading channels in Section V. In Section VI, simulation results are conducted to confirm our theoretical analysis. Finally, in Section VII, conclusions are drawn, and detailed mathematical derivations of the proposed performance analyses are reported in Appendices A and B.

II. Modeling Assumptions

Consider the baseband representation of a linearly modulated signal transmitted through a flat-fading channel. The receiver output is expressed as[1] (see, e.g., [6] and [7])

$$x_c(t) = \mu_c(t)e^{2i\pi f_e t}\sum_l w(l)h_c(t-\epsilon T - lT) + v_c(t) \quad (1)$$

where

$\mu_c(t)$	fading-induced noise;
$\{w(l)\}$	sequence of zero-mean unit variance independently and identically distributed (i.i.d.) symbols;
$h_c(t)$	convolution of the transmitter's signaling pulse and the receiver filter;
$v_c(t)$	complex-valued additive noise;
T	symbol period;
f_e and ϵ	carrier frequency offset and symbol timing delay, respectively, and represent the parameters to be estimated by exploiting the second-order cyclostationary-statistics of the received waveform.

By fractionally oversampling the received signal $x_c(t)$ [see (1)] with the sampling period[2] $T_s := T/P$ ($P \geq 2$), the following discrete-time channel model is obtained:

$$x(n) = \mu(n)e^{2i\pi f_e T n/P}\sum_l w(l)h(n-lP) + v(n) \quad (2)$$

[1]The subscript c is used to denote a continuous-time signal.

[2]The notation $:=$ stands for *is defined as*.

Manuscript received July 5, 2001; revised May 31, 2002. This work was supported by the National Science Foundation under Grant CCR-0092901 and TITF. This work was published, in part, at ICASSP'2001. The associate editor coordinating the review of this paper and approving it for publication was Dr. Chong-Yung Chi.

Y. Wang and E. Serpedin are with the Department of Electrical Engineering, Texas A&M University, College Station, TX 77843 USA (e-mail: serpedin@ee.tamu.edu).

P. Ciblat is with Ecole Nationale Supérieure des Télécommunications, Paris, France.

P. Loubaton is with the Laboratoire Système de Communication, Université de Marne-la-Vallée, Noisy le Grand, France.

Publisher Item Identifier 10.1109/TSP.2002.801919.

where $x(n) := x_c(nT_s)$, $\mu(n) := \mu_c(nT_s)$, $v(n) := v_c(nT_s)$, and $h(n) := h_c(nT_s - \epsilon T)$. In order to derive the asymptotic performance of estimators [6], [7], without any loss in generality, we assume the following:

- **AS1)** $w(n)$ is a zero-mean i.i.d. sequence with values drawn from a linearly modulated complex constellation with unit variance, i.e., $\sigma_w^2 := \mathrm{E}\{|w(n)|^2\} = 1$.
- **AS2)** $\mu(n)$ is a constant fading-induced noise with unit power. Later on, this assumption will be relaxed by considering that $\mu(n)$ is a time-selective fading process.
- **AS3)** $v(n)$ is a complex-valued zero-mean Gaussian process independent of $w(n)$, with variance σ_v^2.
- **AS4)** The combined filter $h_c(t)$ is a raised cosine pulse of bandwidth $[-(1+\rho)/2T, (1+\rho)/2T]$, where the parameter ρ represents the roll-off factor ($0 \leq \rho < 1$) [12, ch. 9].
- **AS5)** Frequency offset f_e is small enough so that the mismatch of the receive filter due to f_e can be neglected [7]. Generally, the condition $f_eT < 0.2$ is assumed. This assumption is required to ensure the validity of channel models (1) and (2).

Based on these assumptions, in the ensuing section, we introduce the nondata-aided estimators of f_e and ϵ proposed in [6] (GSD) and [7] (GG).

III. Frequency Offset and Symbol Timing Estimators for Time-Invariant Channels

A. Usual Definitions

In this paper, the time-varying correlation of the nonstationary process $x(n)$ is defined as

$$r_x(n;\tau) := \mathrm{E}\{x^*(n)x(n+\tau)\}$$

where τ is an integer lag, and the superscript $*$ stands for complex conjugation. By exploiting (2) and taking into account the assumptions **AS1)**–**AS3)**, straightforward calculations lead to

$$r_x(n;\tau) = r_x(n+P;\tau), \qquad \forall\, n, \tau.$$

Being periodic, $r_x(n;\tau)$ admits a Fourier Series expansion

$$r_x(n;\tau) = \sum_{k=0}^{P-1} R_x(k;\tau)e^{2i\pi(kn/P)}$$

whose Fourier's coefficients, which are also termed cyclic correlations, are given for $k = 0, \ldots, P-1$ by the following expression [6], [7]:

$$R_x(k;\tau) := \frac{1}{P}\sum_{n=0}^{P-1} r_x(n;\tau)e^{-2i\pi(kn/P)}.$$

The frequencies k/P (or simply k), for $k = 0, \ldots, P-1$, are referred to as cyclic frequencies or cycles [5]. Furthermore, from these cyclic correlations, it is usual to define a cyclic spectrum for each cyclic frequency k as

$$S_{2,x}(k;f) := \sum_{\tau} R_x(k;\tau)e^{-2i\pi\tau f}. \tag{3}$$

We also define the conjugate second-order time-varying correlation of $x(n)$ as

$$\tilde{r}_x(n;\tau) := \mathrm{E}\{x(n)x(n+\tau)\}.$$

It is easy to check that $\tilde{r}_x(n;\tau)$ can be expressed as

$$\tilde{r}_x(n;\tau) = \sum_{k=0}^{P-1} \tilde{R}_x(k;\tau)e^{2i\pi((k+2f_eT)n/P)}$$

and the conjugate cyclic correlation $\tilde{R}_x(k;\tau)$ can be obtained by the generalized Fourier series expansion [5]

$$\tilde{R}_x(k;\tau) := \lim_{N\to\infty}\frac{1}{N}\sum_{n=0}^{N-1}\tilde{r}_x(n;\tau)e^{-2i\pi((k+2f_eT)n/P)}.$$

Similarly to (3), we can define the conjugate cyclic spectrum $\tilde{S}_{2,x}(k;f)$ as the Fourier transform (FT) of the sequence $\{\tilde{R}_x(k;\tau)\}_\tau$.

In practice, the cyclic correlations $R_x(k;\tau)$ have to be estimated from a finite number of samples N, and the standard sample estimate of $R_x(k;\tau)$ is given by (see, e.g., [4], [5], [7])

$$\hat{R}_x(k;\tau) = \frac{1}{N}\sum_{n=0}^{N-\tau-1} x^*(n)x(n+\tau)e^{-2i\pi(kn/P)}, \quad \tau \geq 0.$$

B. Closed-Form Expressions for the Second-Order Statistics

We now focus on the closed-form expressions of the second-order statistics of the received signal obeying the model (2).

According to (2), we obtain

$$R_x(k;\tau) = \frac{\sigma_w^2}{P}e^{2i\pi(f_eT\tau/P)} \cdot\left(\sum_n h^*(n)h(n+\tau)e^{-2i\pi(kn/P)}\right) + \sigma_v^2 h_c(\tau)\delta(k) \tag{4}$$

where $\delta(.)$ stands for the Kronecker's delta. In order to show the dependency of $R_x(k;\tau)$ on the timing delay ϵ, which is hidden in the expression of the discrete-time channel $h(n)$, an alternative expression for $R_x(k;\tau)$ is next derived, based on the Parseval's relation.

First, the sum in (4) can be rewritten as

$$\sum_n h^*(n)h(n+\tau)e^{-2i\pi(kn/P)} = \int_{-(1/2)}^{1/2} H^*(f)H\left(f+\frac{k}{P}\right)e^{2i\pi(f+(k/P))\tau}\,df$$

where $H(f)$ denotes the FT of $h(n)$. In a similar way [see (4)], we obtain

$$\tilde{R}_x(k,\tau) = \frac{\sigma_{c,w}^2}{P}e^{2i\pi(f_eT\tau/P)} \cdot\left(\sum_n h(n)h(n+\tau)e^{-2i\pi(kn/P)}\right)$$

where $\sigma_{c,w}^2 := E\{w^2(n)\}$.

In order to point out the influence of the oversampling factor, we wish to express the cyclic correlations w.r.t. the continuous-time filter $h_c(t)$. Since the bandwidth of $h_c(t)$ is less than $1/T$ and the oversampling rate is equal to or larger than $2/T$, the oversampling does not introduce any aliasing for Fourier transform of $h(n)$. Therefore, thanks to Poisson's sum, it follows that for $|f| \leq 1/2$ [11, ch. 3]

$$\forall\, P \geq 2, \quad H(f) = \frac{1}{T_s}\, H_c\left(\frac{f}{T_s}\right) e^{-2i\pi f P\epsilon} \tag{5}$$

where $H_c(F)$ stands for the FT of $h_c(t)$. As shown in [6] and [7], we can also express $H(f + k/P)$ for $|f| \leq 1/P$, and $k = \pm 1$ (the cycle $k = -1$ is equivalent to $k = P - 1$ by periodicity) as

$$\forall\, P \geq 3, \quad H(f + k/P) = \frac{1}{T_s}\, H_c\left(\frac{f + k/P}{T_s}\right) \cdot e^{-2i\pi(f + (k/P))P\epsilon}. \tag{6}$$

Based on the previous equations, we can obtain the following formula for $\forall\, P \geq 3$ [7]:

$$R_x(k;\tau) = \frac{\sigma_w^2}{P}\, e^{2i\pi(f_e T\tau/P)} e^{i\pi(k\tau/P)} \cdot e^{-2i\pi k\epsilon} G(k;\tau) + \sigma_v^2 h_c(\tau)\delta(k) \tag{7}$$

where

$$G(k;\tau) := \frac{P}{T}\int_{-P/2T}^{P/2T} H_c\left(F - \frac{k}{2T}\right) H_c\left(F + \frac{k}{2T}\right) \cdot e^{2i\pi(\tau TF/P)}\, dF.$$

Unlike [6] and [7], we have observed that (6) cannot be used in the case when $P = 2$. Indeed, if $P = 2$, then the aliasing effects due to frequency shifting have to be taken into account. Therefore, (7) no longer holds, except for $k = 0$. For $P = 2$ and $|f| \leq 1/2$, the Poisson's sum leads to

$$H\left(f + \frac{1}{2}\right) = \frac{1}{T_s}\left[H_c\left(\frac{f + 1/2}{T_s}\right) e^{-2i\pi\epsilon} + H_c\left(\frac{f - 1/2}{T_s}\right) e^{2i\pi\epsilon}\right] \cdot e^{-4i\pi f\epsilon}.$$

For $P = 2$ and $k = 1$, it follows that

$$R_x(k;\tau) = \sigma_w^2 e^{i\pi(f_e T + 1)\tau} \cos\left[2\pi\left(\epsilon + \frac{\tau}{4}\right)\right] G'(k;\tau) \tag{8}$$

where

$$G'(k;\tau) := \frac{2}{T}\int_{-1/2T}^{1/2T} H_c\left(F - \frac{k}{2T}\right) H_c\left(F + \frac{k}{2T}\right) \cdot e^{i\pi\tau TF}\, dF.$$

Due to the symmetry property of the raised-cosine function $h_c(t)$, one can notice that $H_c(F)$ is a real-valued even function [12, p. 546]. Then, it is easy to check that $G(k;\tau)$ and $G'(k;\tau)$ are real-valued functions. Moreover, due to the bandlimited property of the filter $h_c(t)$, $G(k;\tau)$ and $G'(k;\tau)$ are nonzero only for cycles $k = 0, \pm 1$. In the same way, since $x(n)$ is given by the (2), it is well known that the cyclic spectrum of $x(n)$ can be expressed for $k \neq 0$ as (cf. [17])

$$S_{2,x}(k;\, f) = \frac{\sigma_w^2}{P}\, H(f - f_e T_s) H^*(f - f_e T_s - k/P). \tag{9}$$

It follows that the supports of the functions $f \to H(f - f_e T_s)$ and $f \to H^*(f - f_e T_s - k/P)$ are disjoint as far as the cycles $|k| > 1$, which leads to no cyclic correlation information [$|S_{2,x}(k;\, f)| = 0, \forall\, f$, and hence, $|R_x(k;\tau)| = 0$ for $|k| > 1$]. In a similar way, the conjugate cyclic spectrum can be expressed as

$$\tilde{S}_{2,x}(k;\, f) = \frac{\sigma_{c,w}^2}{P}\, H(f - f_e T_s) H(f_e T_s + k/P - f).$$

C. GG and GSD Estimators

The GG estimator determines the frequency offset f_e and the timing delay ϵ based on the following equations [7, Eqs. (24) and (25)]

$$\begin{cases} \hat{f}_e = \dfrac{P}{4\pi T\tau} \arg\{\hat{R}_x(1;\tau)\hat{R}_x(-1;\tau)\}, & \text{for } P \geq 2 \\ \hat{\epsilon} = -\dfrac{1}{2\pi} \arg \left\{\hat{R}_x(1;\tau) e^{-2i\pi(\hat{f}_e T + 1/2)\tau/P}\right\}, & \text{for } P \geq 3 \\ \hat{\epsilon} = \dfrac{1}{2\pi} \arccos \left\{\mathrm{re}\left(\dfrac{\hat{R}_x(1;\tau) e^{-i\pi(\hat{f}_e T + 1)\tau}}{\sigma_w^2 G'(1;\tau)}\right)\right\} - \dfrac{\tau}{4}, & \text{for } P = 2. \end{cases} \tag{10}$$

The last equation in the array (10) represents the right form of the GG symbol timing delay estimator in the case when $P = 2$, and its expression follows directly from (8).

Note that the estimator presented in [14] can be obtained by choosing $\tau = P$ in (10). As described in [6], the performance of the frequency offset and timing delay estimators does not change significantly w.r.t. τ. Therefore, for sake of clarity, throughout this paper, we choose $\tau = 1$ for the GG estimator. In this case, one can see that the GSD frequency offset estimator [6, Eq. (7)] coincides with the GG algorithm. Consequently, it is sufficient to analyze the GG frequency offset estimator. In contrast, the timing delay estimator corresponding to the GSD algorithm [6, Eq. (8)] is different than the GG symbol timing delay estimator and is given by

$$\begin{cases} \hat{\epsilon} = -\dfrac{1}{2\pi} \arg\{\hat{R}_x(1;0)\}, & \text{for } P \geq 3 \\ \hat{\epsilon} = \dfrac{1}{2\pi} \arccos\left\{\mathrm{re}\left(\dfrac{\hat{R}_x(1;0)}{\sigma_w^2 G'(1;0)}\right)\right\}, & \text{for } P = 2. \end{cases} \tag{11}$$

In the next section, we establish the asymptotic variances of estimators (10) and (11), which are defined as

$$\gamma_{f_e} := \lim_{N\to\infty} N\mathrm{E}\left\{(\hat{f}_e - f_e)^2\right\}$$

$$\gamma_{\epsilon} := \lim_{N\to\infty} N\mathrm{E}\left\{(\hat{\epsilon} - \epsilon)^2\right\}.$$

IV. Performance Analysis for Time-Invariant Channels

In order to establish the asymptotic variance of the asymptotically unbiased and consistent estimators (10) and (11), it is necessary to evaluate the normalized unconjugate/conjugate asymptotic covariances of the cyclic correlations, which are defined as

$$\begin{aligned}\mathbf{\Gamma}_{u,v}^{(k,l)} &= \lim_{N\to\infty} N\mathrm{E} \\ &\quad \cdot\left\{(\hat{R}_x(k;u)-R_x(k;u))(\hat{R}_x(l;v)-R_x(l;v))^*\right\} \\ \tilde{\mathbf{\Gamma}}_{u,v}^{(k,l)} &= \lim_{N\to\infty} N\mathrm{E} \\ &\quad \cdot\left\{(\hat{R}_x(k;u)-R_x(k;u))(\hat{R}_x(l;v)-R_x(l;v))\right\}.\end{aligned}$$

As the estimators (10) and (11) are dealing only with the cyclic correlations at cycles $k=\pm 1$, in the sequel, we concentrate on the derivation of the asymptotic covariances of the cyclic correlations for $k,\, l=\pm 1$. According to [1], we obtain

$$R_x(k;\tau)=e^{2i\pi(k\tau/P)}R_x^*(-k;-\tau)$$

which implies that

$$\tilde{\mathbf{\Gamma}}_{u,v}^{(k,l)}=e^{2i\pi(lv/P)}\mathbf{\Gamma}_{u,-v}^{(k,-l)}. \tag{12}$$

Thus, it is sufficient to evaluate $\mathbf{\Gamma}$ since $\tilde{\mathbf{\Gamma}}$ can be obtained directly based on (12). In [2] and [20], $\mathbf{\Gamma}^{(1,1)}$ and $\tilde{\mathbf{\Gamma}}^{(1,1)}$ are obtained only for circular input sequences (i.e., input sequences that satisfy the condition $\mathrm{E}\{w(n)w(n+\tau)\}=0$). The following proposition, which is an extension of the results presented in [2] and [20], is established in Appendix A.

Proposition 1: The asymptotic variances of the cyclic correlation estimates are given by

$$\begin{aligned}\mathbf{\Gamma}_{u,v}^{(1,1)} &= \sum_{k=0}^{P-1} e^{2i\pi(kv/P)}\int_0^1 S_{2,x}(k;f)S_{2,x}^*\left(k;f-\frac{1}{P}\right) \\ &\quad \cdot e^{2i\pi(u-v)f}\,df+\sum_{k=0}^{P-1} e^{-2i\pi((1+k+2f_eT)v/P)} \\ &\quad \cdot\int_0^1 \tilde{S}_{2,x}(k;f)\tilde{S}_{2,x}^*\left(k;f-\frac{1}{P}\right) \\ &\quad \cdot e^{2i\pi(u+v)f}\,df+\kappa PR_x(1;u)R_x^*(1;v) \\ \mathbf{\Gamma}_{u,v}^{(1,-1)} &= \sum_{k=0}^{P-1} e^{2i\pi(kv/P)}\int_0^1 S_{2,x}(k;f)S_{2,x}^*\left(k-z;f-\frac{1}{P}\right) \\ &\quad \cdot e^{2i\pi(u-v)f}\,df+\sum_{k=0}^{P-1} e^{2i\pi((1-k-2f_eT)v/P)} \\ &\quad \cdot\int_0^1 \tilde{S}_{2,x}(k;f)\tilde{S}_{2,x}^*\left(k-2;f-\frac{1}{P}\right) \\ &\quad \cdot e^{2i\pi(u+v)f}\,df+\kappa PR_x(1;u)R_x^*(-1;v)\end{aligned}$$

$$\mathbf{\Gamma}_{u,v}^{(-1,1)}=\mathbf{\Gamma}_{v,u}^{*(1,-1)},\quad \mathbf{\Gamma}_{u,v}^{(-1,-1)}=e^{2i\pi((v-u)/P)}\mathbf{\Gamma}_{-v,-u}^{(1,1)}$$

and κ denotes the kurtosis of $w(n)$.

In the above proposition, some terms within the sums may cancel out. Indeed, since the filter $h_c(t)$ is bandlimited, the cyclic spectra at cycles $|k|>1$ are zero. This remark implies, for example, that if $P>4$, then only the terms driven by the index $k=0$ remain in the expression of $\mathbf{\Gamma}^{(1,1)}$ and $k=1$ in $\mathbf{\Gamma}^{(1,-1)}$. When $P=2$, only $\mathbf{\Gamma}^{(1,1)}$ is needed since $R_x(1;\tau)=R_x(-1;\tau)$.

A. Performance Analysis of the GG Estimator

The asymptotic performance of the GG estimator is established in Appendix B. The following proposition sums up the expressions of the asymptotic variance of the GG frequency offset estimator.

Proposition 2: For $P\geq 3$, the asymptotic variance of the frequency offset estimator (10) is given by[3]

$$\gamma_{f_e}=\frac{P^4\left(\mathbf{\Psi}^T\mathbf{\Gamma}\mathbf{\Psi}^*-\mathrm{re}\left\{e^{-4i\pi f_eT/P}\mathbf{\Psi}^T\tilde{\mathbf{\Gamma}}\mathbf{\Psi}\right\}\right)}{32\pi^2T^2\sigma_w^4G^2(1;1)}$$

where

$$\mathbf{\Psi}=[\psi,\ \psi^*]^T,\quad \psi=e^{2i\pi(\epsilon-1/2P)}$$

$$\mathbf{\Gamma}=\begin{bmatrix}\mathbf{\Gamma}_{1,1}^{(1,1)} & \mathbf{\Gamma}_{1,1}^{(1,-1)}\\ \mathbf{\Gamma}_{1,1}^{(-1,1)} & \mathbf{\Gamma}_{1,1}^{(-1,-1)}\end{bmatrix}$$

and $\tilde{\mathbf{\Gamma}}$ is defined in a similar way as $\mathbf{\Gamma}$.

For $P=2$, the asymptotic variance of the frequency offset estimator (10) is given by

$$\gamma_{f_e}=\frac{\mathbf{1}^T\mathbf{\Gamma}\mathbf{1}-\mathrm{re}\left\{e^{-2i\pi f_eT}\mathbf{1}^T\tilde{\mathbf{\Gamma}}\mathbf{1}\right\}}{8\pi^2T^2\sigma_w^4\sin^2(2\pi\epsilon)G'^2(1;1)}$$

where $\mathbf{1}=[1,\,1]^T$.

The closed-form expression of the GG timing symbol delay estimator is drawn in the following proposition.

Proposition 3: For $P\geq 3$, the asymptotic variance of the timing delay estimator (10) is given by

$$\gamma_\epsilon=\frac{P^2\mathrm{re}\left\{e^{-4i\pi f_\epsilon T/P}\tilde{\mathbf{\Gamma}}_{1,1}^{(1,-1)}-\psi^2\mathbf{\Gamma}_{1,1}^{(1,-1)}\right\}}{8\pi^2\sigma_w^4G^2(1;1)}+\frac{T^2}{P^2}\gamma_{f_e}.$$

For $P=2$, the asymptotic variance of the timing delay estimator (10) is given by

$$\gamma_\epsilon=\frac{\mathbf{\Gamma}_{1,1}^{(1,1)}+\mathrm{re}\left\{e^{-2i\pi f_eT}\tilde{\mathbf{\Gamma}}_{1,1}^{(1,1)}\right\}}{8\pi^2\sigma_w^4\cos^2(2\pi\epsilon)G'^2(1;1)}.$$

B. Performance Analysis of the GSD Estimator

When compared with the GG algorithm (10), the symbol timing delay estimators corresponding to the GSD algorithm are obtained from (11) and by fixing $\tau=0$. Note that such a choice of τ decouples the symbol timing delay estimators from the frequency offset estimator in the sense that the estimation of ϵ does not require an initial estimate of f_e [6]. The following result holds.

Proposition 4: For $P\geq 3$, the asymptotic variance of the timing delay estimator (11) is given by

$$\gamma_\epsilon=\frac{P^2\left(\mathbf{\Gamma}_{0,0}^{(1,1)}-\mathrm{re}\left\{e^{4i\pi\epsilon}\tilde{\mathbf{\Gamma}}_{0,0}^{(1,1)}\right\}\right)}{8\pi^2\sigma_w^4G^2(1;0)}.$$

[3]The notations re and im stand for the real and imaginary part, respectively.

For $P = 2$, the asymptotic variance of the timing delay estimator (11) is given by

$$\gamma_\epsilon = \frac{\mathbf{\Gamma}_{0,0}^{(1,1)} + \mathrm{re}\left\{\tilde{\mathbf{\Gamma}}_{0,0}^{(1,1)}\right\}}{8\pi^2\sigma_w^4 \sin^2(2\pi\epsilon) G'^2(1;0)}.$$

We note that analyzing theoretically the influence of the system parameters such as oversampling factor or excess bandwidth factor from the equations displayed in the previous propositions is quite difficult. Therefore, we need numerical illustrations to highlight the contribution of each parameter to the performance. These simulation experiments show that selection of larger values for the oversampling factor P does not improve the performance of estimators (10) and (11). In addition, we also notice that the convergence rate of all the estimators (the mean-square error) decreases proportionally with $1/N$, where N stands for the number of available observations. In particular, the frequency offset estimators (10) and (11) converge slower than the estimator described in [3], which exploits the conjugate cyclostationary statistics of the received waveform.

V. Extension to Time-Selective Channels

Due to the assumption **AS2)**, the foregoing discussion applies only to time-invariant channels. In this section, we will see that the results obtained in the Section IV can be extended to the case of time-selective fading effects as long as the fading distortion $\mu_c(t)$ is approximately constant over a pulse duration or, equivalently, the Doppler spread $B_\mu T$ is small, where B_μ denotes the bandwidth of $\mu_c(t)$ [7].

Assuming now that $\mu(n)$ is a stationary complex process with autocorrelation $r_\mu(\tau) := \mathrm{E}\{\mu^*(n)\mu(n+\tau)\}$ [7], we can rewrite (4) for $k = \pm 1$ as

$$R_x(k;\tau) = \frac{\sigma_w^2}{P} r_\mu(\tau) e^{2i\pi(f_\epsilon T\tau/P)} \sum_n h^*(n)h(n+\tau) \cdot e^{-2i\pi(kn/P)}. \quad (13)$$

Based on (13), it is not difficult to find that all the previous estimators [see (10) and (11)] still hold true, except that for $P = 2$, they take the form

$$\hat{\epsilon} = \frac{1}{2\pi}\arccos\left\{\mathrm{re}\left(\frac{\hat{R}_x(1;1)e^{-i\pi(\hat{f}_\epsilon T+1)}}{\sigma_w^2 G'(1;1) r_\mu(1)}\right)\right\} - \frac{1}{4}$$

$$\hat{\epsilon} = \frac{1}{2\pi}\arccos\left\{\mathrm{re}\left(\frac{\hat{R}_x(1;0)}{\sigma_w^2 G'(1;0) r_\mu(0)}\right)\right\} \quad (14)$$

respectively.

Compared with the performance analysis reported in Section IV, the exact asymptotic variance of GG and GSD estimators in the case of time-selective channels supports several modifications. We now introduce an additional assumption on the fading channel.

AS6) The land-mobile channel is a Rayleigh fading channel, which means that $\mu(n)$ is a zero-mean complex-valued circular Gaussian process [12].

For general land-mobile channel models, the autocorrelation of $\mu(n)$ is proportional to the zero-order Bessel function, i.e., $r_\mu(\tau) \propto J_0(2\pi B_\mu \tau)$ (cf. [13]). Based on the assumption **AS6)**, $\tilde{r}_x(n;\tau) = 0$ and the higher order cumulants of $x(n)$ are also zero. Therefore, following the steps of Appendices A and B, one can find that in the presence of time-selective fading effects, the performance analysis can be established in a similar way as in the case of time-invariant fading channels. In fact, considering the assumption **AS6)**, only the first terms of $\mathbf{\Gamma}_{u,v}^{(1,1)}$ and $\mathbf{\Gamma}_{u,v}^{(1,-1)}$ in Proposition 1 survive, and the asymptotic variances γ_{f_ϵ} and γ_ϵ for the GG and GSD estimators in Propositions 2–4 still hold true, except that some constants related to $r_\mu(1)$ or $r_\mu(0)$ should be added. For example, when $P = 2$, based on (14), we now obtain the following expressions for the asymptotic variances corresponding to the GG and GSD timing delay estimators:

$$\gamma_\epsilon = \frac{\mathbf{\Gamma}_{1,1}^{(1,1)} + \mathrm{re}\left\{e^{-2i\pi f_\epsilon T}\tilde{\mathbf{\Gamma}}_{1,1}^{(1,1)}\right\}}{8\pi^2\sigma_w^4 \cos^2(2\pi\epsilon) G'^2(1;1) r_\mu^2(1)}$$

$$\gamma_\epsilon = \frac{\mathbf{\Gamma}_{0,0}^{(1,1)} + \mathrm{re}\left\{\tilde{\mathbf{\Gamma}}_{0,0}^{(1,1)}\right\}}{8\pi^2\sigma_w^4 \sin^2(2\pi\epsilon) G'^2(1;0) r_\mu^2(0)}$$

respectively.

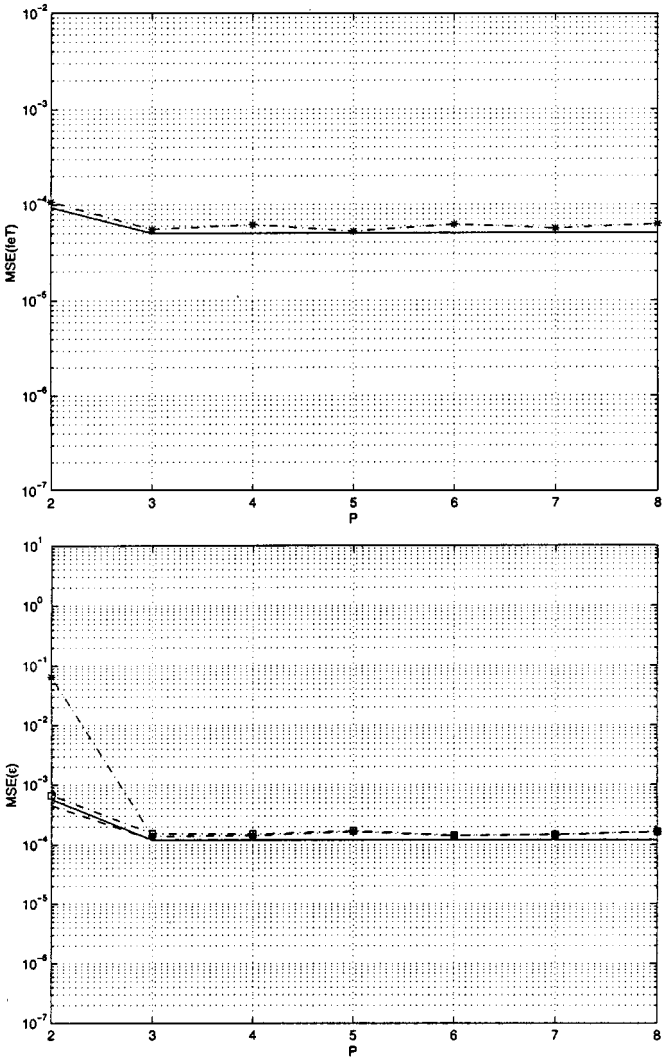

Fig. 1. GG/GSD estimators. MSE of $\widehat{f_\epsilon T}$ and $\hat{\epsilon}$ versus P for BPSK and time-invariant channel.

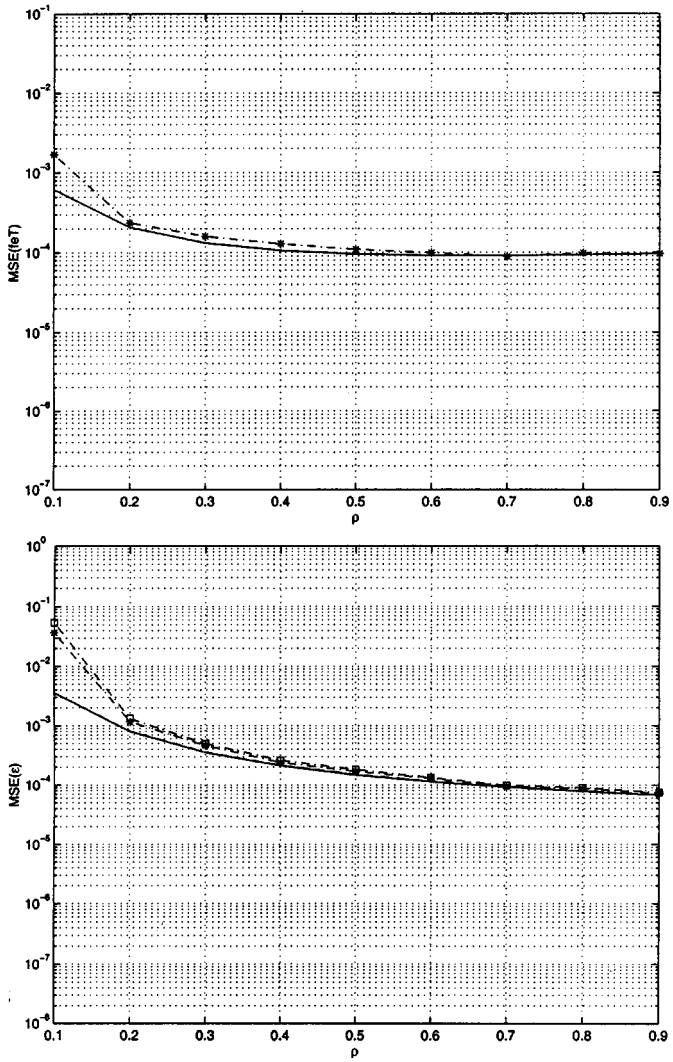

Fig. 2. GG/GSD estimators. MSE of $\widehat{f_\epsilon T}$ and $\hat{\epsilon}$ versus ρ for BPSK and time-invariant channel.

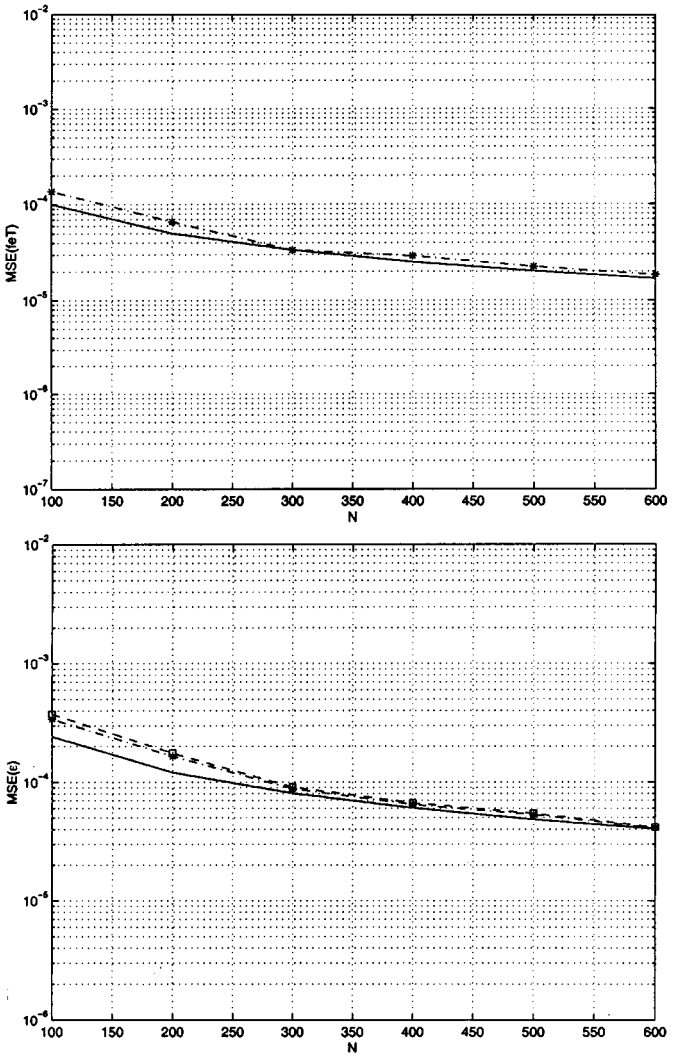

Fig. 3. GG/GSD estimators. MSE of $\widehat{f_\epsilon T}$ and $\hat{\epsilon}$ versus N for BPSK and time-invariant channel.

In closing this section, it is interesting to remark that for implementing the GG and GSD frequency-offset estimators, no information regarding the time-varying fading process $\mu(n)$ is required. If the oversampling factor satisfies $P \geq 3$, then the implementation of the GG and GSD timing delay estimators also requires no knowledge of $\mu(n)$. However, when $P = 2$, knowledge of the second-order statistics $r_\mu(0)$ and $r_\mu(1)$ is required to implement the GG and GSD timing delay estimators (14). However, simulation experiments, which are reported in the next section, show that from a computational complexity and performance viewpoint, the best value of the oversampling factor is $P = 3$. Thus, estimation of parameters $r_\mu(0)$ and $r_\mu(1)$ can be avoided by selecting $P > 2$.

VI. Simulation Experiments

In this section, the experimental mean-square error (MSE) results and theoretical asymptotic bounds of estimators (10) and (11) are compared. The experimental results are obtained by performing a number of 400 Monte Carlo trials, assuming that the transmitted symbols are i.i.d. linearly modulated symbols with $\sigma_w^2 = 1$. The transmit and receive filters are square-root raised cosine filters, and the additive noise $v(n)$ is generated by passing a Gaussian white noise through the square-root raised cosine filter to yield a discrete-time noise sequence with autocorrelation sequence $r_v(\tau) := \mathrm{E}\{v^*(n)v(n+\tau)\} = \sigma_v^2 h_c(\tau)$ [7]. The signal-to-noise ratio (SNR) is defined as SNR:= $10\log_{10}(\sigma_w^2/\sigma_v^2)$. Experiments 1 to 4 assume BPSK symbols transmitted through time-invariant channels, whereas Experiments 5 to 6 are performed assuming time-selective Rayleigh fading and QPSK constellations. In our simulations, the Doppler spread is set to $B_\mu T = 0.005$ (very slow fading), and $\mu(n)$ is created by passing a unit-power zero-mean white Gaussian noise process through a normalized discrete-time filter, which is obtained by bilinearly transforming a third-order continuous-time all-pole filter, whose poles are the roots of the equation $(s^2 + 0.35\omega_0 s + \omega_0^2)(s + \omega_0) = 0$, where $\omega_0 = 2\pi B_\mu / 1.2$.

In all figures, the theoretical bounds of GG and GSD estimators are represented by the solid line and the dash line, respectively. The experimental results of GG and GSD estimators are plotted using dash-dot lines with stars and squares, respectively. Since the frequency offset estimators of GG and GSD are equivalent, only the former will be presented.

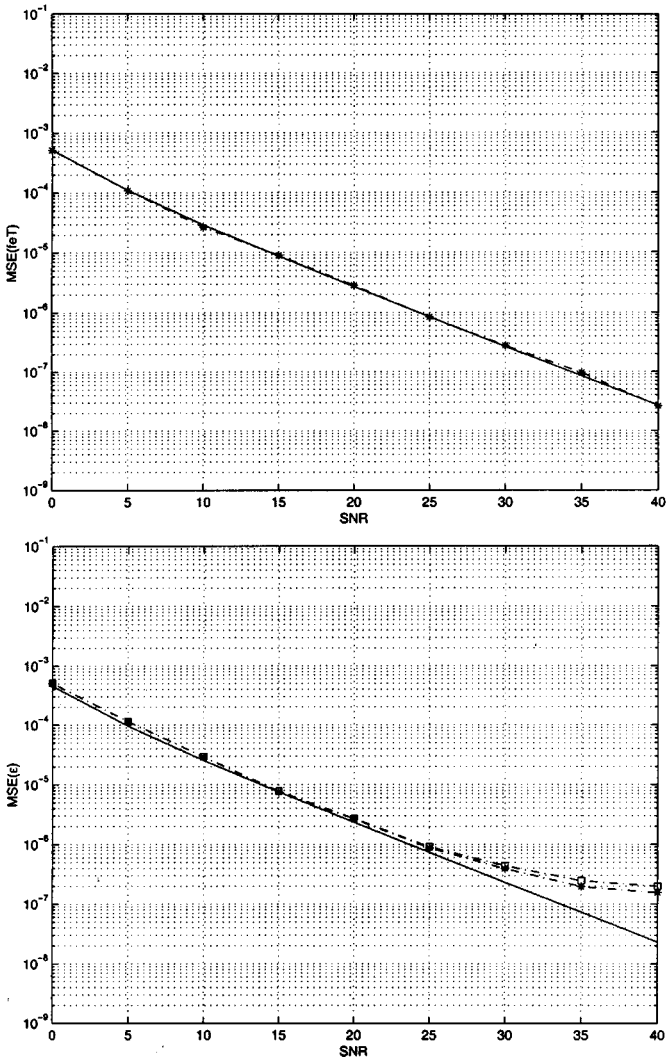

Fig. 4. GG/GSD estimators. MSE of $\widehat{f_eT}$ and $\hat{\epsilon}$ versus SNR for BPSK and time- invariant channel.

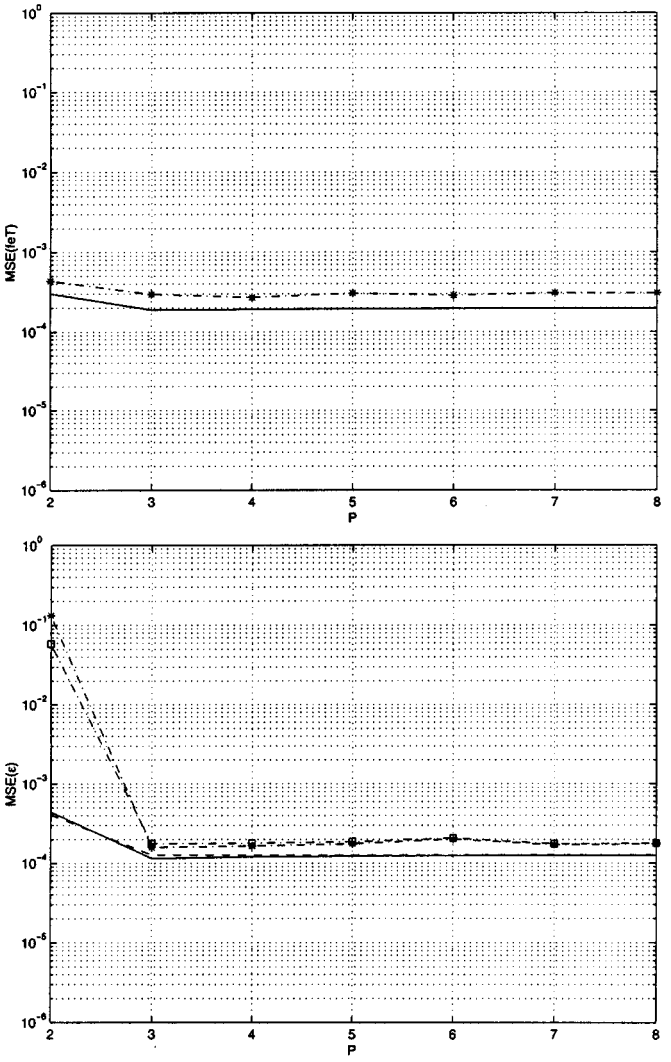

Fig. 5. GG/GSD estimators. MSE of $\widehat{f_eT}$ and $\hat{\epsilon}$ versus P for QPSK and time-selective channel.

Experiment 1—Performance Versus the Oversampling Rate P for BPSK Constellation: By varying the oversampling rate P, we compare the MSE of GG and GSD estimators with their theoretical asymptotic variances. The number of symbols is set to $N = 200$, the roll-off factor of the pulse shape is $\rho = 0.5$, and SNR $= 10$ dB. The normalized frequency offset and timing delay are $f_eT = 0.05$ and $\epsilon = 0.37$, respectively. The results are depicted in Fig. 1. It turns out that increasing the oversampling rate does not improve performance of the frequency offset and timing delay estimators as long as $P \geq 3$. This is a result that may be predicted by Shannon interpolation theorem, and since the estimators (10) and (11) exploit the second-order statistics of the received signal $x(n)$, an oversampling rate larger than 2 is necessary to make the cyclic spectra alias-free [8], [10]. Moreover, although more samples are collected as P increases, their correlation increases as well, which is known to increase the variance of the estimators [7].

Experiment 2—Performance Versus the Filter Bandwidth for BPSK Constellation: Fig. 2 depicts the MSE of the estimators versus the roll-off factor ρ, assuming oversampling rate $P = 4$, $N = 200$ transmitted symbols, SNR $= 10$ dB, $f_eT = 0.1$, and $\epsilon = 0.37$. It can be seen that with ρ increasing, the performance of the timing delay estimators improves. This is an expected property since physically, wideband pulses have comparatively short duration and, therefore, are better "seen" in the presence of noise [9, p. 65]. From another viewpoint, based on (9) and since $h_c(t)$ is bandlimited, it follows that as the bandwidth decreases, the second-order cyclic spectra are numerically weak, i.e., less cyclic correlation information is available.

Experiment 3—Performance Versus the Number of Input Symbols N for BPSK Constellation: In Fig. 3, the theoretical and experimental MSE of the frequency offset and symbol timing delay estimators are plotted versus the number of symbols N, assuming the following parameters: $P = 4$, $\rho = 0.5$, SNR$=$ 10 dB, $f_eT = 0.05$, and $\epsilon = 0.37$. Fig. 3 shows that the experimental MSE of all the estimators are well predicted by the theoretical bounds derived in Section IV.

Experiment 4—Performance Versus SNR for BPSK Constellation: Fig. 4 depicts the experimental and theoretical MSE of the GG and GSD estimators versus SNR, assuming the parameters $P = 4$, $\rho = 0.9$, $N = 500$, $f_eT = 0.05$, and $\epsilon = 0.37$. The simulation results of timing estimators for high SNR range are

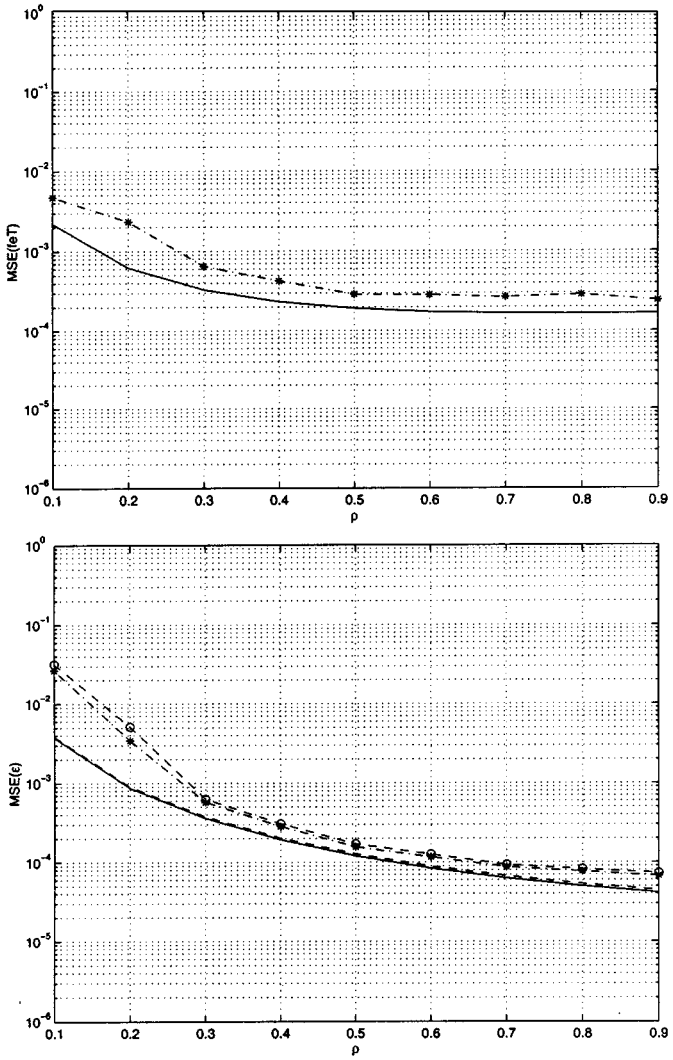

Fig. 6. GG/GSD estimators. MSE of $\widehat{f_eT}$ and $\hat{\epsilon}$ versus ρ for QPSK and time-selective channel.

supposed to agree with the theoretical bounds when the number of samples N is sufficiently large to make the self noise negligible (cf. [9, ch. 6]).

Experiment 5—Performance Versus the Oversampling Rate P in Time-Selective Channels for QPSK Constellation: We repeat Experiment 1 by assuming QPSK symbols passing through a time-selective channel. The number of symbols is set to $N = 400$, the roll-off factor of the pulse shape is $\rho = 0.5$, SNR $=$ 10 dB, $f_eT = 0.2$, and $\epsilon = 0.37$. The results are depicted in Fig. 5. It turns out again that when $P \geq 3$, the performance of GG and GSD estimators does not depend on the oversampling factor P. Therefore, larger oversampling factors ($P = 4, \ldots, 8$) are not justifiable from a computational and performance improvement viewpoint.

Experiment 6—Performance Versus the Filter Bandwidth in Time-Selective Channels for QPSK Constellation: Fig. 6 depicts the MSE of the estimators versus the roll-off factor ρ in the presence of time-varying fading effects, assuming oversampling rate $P = 4$, $N = 400$ transmitted symbols, SNR $= 10$ dB, $f_eT = 0.2$, and $\epsilon = 0.37$. Both the theoretical and experimental results corroborate again the conclusion of Experiment 2. Pulse shapes with larger bandwidths can improve the performance of the timing delay estimators.

VII. Conclusions

In this paper, we have analyzed the asymptotic performance of the blind carrier frequency offset and timing delay estimators introduced in [6] and [7]. Such estimators rely on the second-order cyclostationary statistics generated by oversampling the output of the receive filter. We have derived the asymptotic variance expressions of $\hat{f}_e$ and $\hat{\epsilon}$ and shown that a smaller oversampling rate ($P = 3$) can improve the estimation accuracy as well as reduce the computational complexity of the estimators.

By properly taking into account the aliasing effects, we have shown that when $P = 2$, the timing delay estimators take a different form than the expressions reported in [6] and [7]. In a future paper, we will report the more complex performance analysis of these estimators in the presence of multipath channels.

Appendix A
Derivation of Proposition 1

In [2] and [20], a powerful approach has been developed for calculating the asymptotic covariance matrices of the cyclic correlation estimates. In order to derive $\mathbf{\Gamma}^{(1,1)}$ and $\mathbf{\Gamma}^{(1,-1)}$, we strongly refer to the method introduced in the aforementioned reference.

Define the mean-compensated $(2\Upsilon + 1)$-dimensional stochastic process

$$\mathbf{e}_2(n) = \mathbf{x}_2(n) - \mathbf{r}_x(n)$$

where

$$\mathbf{x}_2(n) = [x(n-\Upsilon)x^*(n), \ldots, x(n+\Upsilon)x^*(n)]^T$$

and

$$\mathbf{r}_x(n) = [r_x(n; -\Upsilon), \ldots, r_x(n; \Upsilon)]^T.$$

Let $\boldsymbol{r}_{\mathbf{e}_2}(n, \tau) := \mathrm{E}\{\mathbf{e}_2(n+\tau)\mathbf{e}_2^{\mathrm{H}}(n)\}$ be the time-varying correlation where the superscript H denotes complex-conjugation and transposition. Furthermore, let $\boldsymbol{R}_{\mathbf{e}_2}(k, \tau)$ and $\boldsymbol{S}_{\mathbf{e}_2}(k; f)$ represent the cyclic correlation and cyclic spectrum of $\mathbf{e}_2(n)$, respectively. In [2] and [20], it is shown that

$$\mathbf{\Gamma}^{(1,1)} = \boldsymbol{S}_{\mathbf{e}_2}(0; 1/P).$$

Based on similar arguments as the ones developed in [2] and [20], it is not difficult to prove that

$$\mathbf{\Gamma}^{(1,-1)} = \boldsymbol{S}_{\mathbf{e}_2}(2; 1/P).$$

Next, we will only concentrate on the derivation of $\mathbf{\Gamma}^{(1,1)}$. The derivation of $\mathbf{\Gamma}^{(1,-1)}$ can be done similarly. First, we characterize the cyclic spectrum of the process $\mathbf{e}_2(n)$. For a general noncircular input, the time-varying correlation of $\mathbf{e}_2(n)$ can be expressed as

$$\begin{aligned}[\boldsymbol{r}_{\mathbf{e}_2}(n; \tau)]_{u,v} &= r_x(n+v; \tau+u-v)r_x^*(n; \tau) \\ &\quad + \mathrm{cum}\{x(n+u+\tau), x^*(n+\tau), x^*(n+v), x(n)\} \\ &\quad + \tilde{r}_x(n; \tau+u)\tilde{r}_x^*(n+v; \tau-v)\end{aligned}$$

where $(u, v) \in \{-\Upsilon, \ldots, \Upsilon\}^2$. Let the notation $[\boldsymbol{M}]_{u,v}$ stand for the (u, v)th entry of an arbitrary matrix $\boldsymbol{M}$. It follows that

the cyclic correlations of $\mathbf{e}_2(n)$ at the cyclic frequency $k = 0$ are given by

$$\begin{aligned}[\boldsymbol{R}_{\mathbf{e}_2}(0;\,\tau)]_{u,\,v} &= \sum_{k=0}^{P-1} R_x(k;\,\tau+u-v)R_x^*(k;\,\tau)e^{2i\pi kv/P} \\ &\quad + C_x(0;\,u+\tau,\,-\tau,\,-v) \\ &\quad + \sum_{k=0}^{P-1} \tilde{R}_x(k;\,\tau+u)\tilde{R}_x^*(k;\,\tau-v)e^{-(2i\pi(k+2f_eT)v/P)}\end{aligned}$$

where the cyclic cumulant sequence $C_x(k;\boldsymbol{\tau}), \boldsymbol{\tau} := [\tau_1,\,\tau_2,\,\tau_3]$ can be expressed as

$$C_x(k;\,\boldsymbol{\tau}) := \int_{-1/2}^{1/2} S_{4,\,x}(k;\,\mathbf{f})e^{2i\pi\boldsymbol{\tau}\mathbf{f}^T}\,d\mathbf{f}$$

where $S_{4,\,x}(k;\,\mathbf{f})$ stands for the cyclic trispectrum of the discrete-time signal $x(n)$ at cyclic frequency k/P and frequency $\mathbf{f} := [f_1,\,f_2,\,f_3]$.

Thus

$$\begin{aligned}\boldsymbol{\Gamma}_{u,\,v}^{(1,\,1)} &= [\boldsymbol{S}_{\mathbf{e}_2}(0;\,1/P)]_{u,\,v} \\ &= \sum_{k=0}^{P-1} \mathcal{R}_{k,\,u,\,v} + \mathcal{C}_{u,\,v} + \sum_{k=0}^{P-1} \tilde{\mathcal{R}}_{k,\,u,\,v}\end{aligned}$$

where

$$\begin{aligned}\mathcal{R}_{k,\,u,\,v} &= e^{2i\pi kv/P}\sum_{\tau\in\mathbb{Z}} R_x(k;\,\tau+u-v)R_x^*(k;\,\tau)e^{-2i\pi\tau/P} \\ \mathcal{C}_{u,\,v} &= \sum_{\tau\in\mathbb{Z}} C_x(0;\,u+\tau,\,-\tau,\,-v)e^{-2i\pi\tau/P} \\ \tilde{\mathcal{R}}_{k,\,u,\,v} &= e^{-(2i\pi(k+2f_eT)v/P)}\sum_{\tau\in\mathbb{Z}} \tilde{R}_x(k;\,\tau+u) \\ &\quad \cdot \tilde{R}_x^*(k;\,\tau-v)e^{-(2i\pi\tau/P)}.\end{aligned}$$

We still need to express $\mathcal{C}_{u,\,v}$. We recall that

$$\begin{aligned}\mathcal{C}_{u,\,v} = \int_{-(1/2)}^{1/2} S_{4,\,x}(0;\,f_1,\,f_2,\,f_3)\sum_{\tau\in\mathbb{Z}} e^{2i\pi(f_1(u+\tau)-f_2\tau-f_3v)} \\ \cdot e^{-(2i\pi\tau/P)}\,df_1\,df_2\,df_3. \quad (15)\end{aligned}$$

Let $S_{4,\,x_c}(k/T;\,\mathbf{F})$ be the cyclic trispectrum of $x_c(t)$ at cyclic frequency k/T and frequency $\mathbf{F} := [F_1,\,F_2,\,F_3]$. From [8], [10], and [16], $S_{4,\,x}(k;\,\mathbf{f})$ can be expressed in terms of $S_{4,\,x_c}(k/T;\,\mathbf{F})$ by

$$\begin{aligned}S_{4,\,x}(k;\,\mathbf{f}) &= \frac{1}{T_s^3}\sum_{l\in\mathbb{Z}}\sum_{\boldsymbol{\mu}\in\mathbb{Z}^3} S_{4,\,x_c}\left(\frac{l}{T};\,\frac{\mathbf{f}-\boldsymbol{\mu}}{T_s}\right)\delta\left(\frac{k-l}{P}\bmod 1\right)\end{aligned}$$

for all $(f_1,\,f_2,\,f_3) \in (-1/2,\,1/2]^3$. The notation $(a \bmod b)$ denotes a modulo b, and by convention, $(a \bmod b)$ belongs to $(-b/2,\,b/2]$.

Since $x_c(t)$ is given by (1), it is well known that (see [2, App. C], [15], and [20])

$$\begin{aligned}S_{4,\,x_c}\left(\frac{k}{T};\,\mathbf{F}\right) = \frac{\kappa}{T}H_c(F_1-f_e)H_c^*(F_2-f_e)H_c^*(F_3-f_e) \\ \cdot H_c\left(\frac{k}{T}-F_1+F_2+F_3-f_e\right)e^{-2i\pi k\epsilon} \quad (16)\end{aligned}$$

where $H_c(F)$ represents the FT of $h_c(t)$. As $h_c(t)$ is bandlimited in $[-(1+\rho)/2T,\,(1+\rho)/2T]$ with $0 \le \rho < 1$, $S_{4,\,x_c}(k/T;\,\mathbf{F})$ will be nonzero only for cycles $\{k/T,\,|k| \le 3\}$. We deduce that

$$\begin{aligned}S_{4,\,x}(k;\,\mathbf{f}) = \frac{1}{T_s^3}\sum_{l=-3}^{3}\sum_{\boldsymbol{\mu}\in\mathbb{Z}^3} S_{4,\,x_c}\left(\frac{l}{T};\,\frac{\mathbf{f}-\boldsymbol{\mu}}{T_s}\right) \\ \cdot\delta\left(\frac{k-l}{P}\bmod 1\right) \quad (17)\end{aligned}$$

for all $(f_1,\,f_2,\,f_3) \in (-1/2,\,1/2]^3$.

According to (15) and (17), we obtain that for $P \ge 3$

$$\begin{aligned}\mathcal{C}_{u,\,v} = \frac{1}{T_s^3}\sum_{\substack{l=-3 \\ l=(0\bmod P)}}^{3}\int_{-(1/2)}^{1/2} S_{4,\,x_c}\left(\frac{l}{T};\,\frac{f_1}{T_s},\,\frac{f_1-1/P}{T_s},\,\frac{f_3}{T_s}\right) \\ \cdot e^{2i\pi(f_1u-f_3v)}\,df_1\,df_3.\end{aligned}$$

Replacing the cyclic spectra of $x_c(t)$ with their expressions given by (16) and then expressing $H_c(F)$ in terms of $H(f)$ by means of (5) leads to

$$\begin{aligned}\mathcal{C}_{u,\,v} = \frac{\kappa T_s}{T}\int_{-(1/2)}^{1/2} H(f_1-f_eT_s)H^*\left(f_1-\frac{1}{P}-f_eT_s\right) \\ \cdot H^*(f_3-f_eT_s)H\left(f_3-\frac{1}{P}-f_eT_s\right)e^{2i\pi(f_1u-f_3v)}\,df_1\,df_3.\end{aligned}$$

Using (9), we finally obtain

$$\begin{aligned}\mathcal{C}_{u,\,v} &= \frac{\kappa T}{T_s}\int_{-(1/2)}^{1/2} S_{2,\,x}(1;\,f_1)e^{2i\pi f_1u}\,df_1\int_{-(1/2)}^{1/2} \\ &\quad \cdot S_{2,\,x}^*(1;\,f_3)e^{-2i\pi f_3v}\,df_3 \\ &= \frac{\kappa T}{T_s}\,R_x(1;\,u)R_x^*(1;\,v).\end{aligned}$$

The expressions in the case of $P = 2$ can be obtained using a similar approach.

Appendix B
Proof of Proposition 2

We establish next the asymptotic performance of the GG estimators for $P \ge 3$. For $\tau = 1$, (10) can be rewritten as

$$\hat{f}_e = \frac{P}{4\pi T}\arg\left\{\hat{R}_x(1;\,1)\hat{R}_x(-1;\,1)\right\} = \frac{P}{4\pi T}\arctan\left\{\frac{\hat{\alpha}_1}{i\hat{\beta}_1}\right\} \quad (18)$$

where

$$\begin{aligned}\hat{\alpha}_1 &:= \hat{R}_x(1;\,1)\hat{R}_x(-1;\,1) - \hat{R}_x^*(1;\,1)\hat{R}_x^*(-1;\,1) \\ \hat{\beta}_1 &:= \hat{R}_x(1;\,1)\hat{R}_x(-1;\,1) + \hat{R}_x^*(1;\,1)\hat{R}_x^*(-1;\,1).\end{aligned}$$

For convenience, we define

$$\begin{aligned}\alpha_1 &:= R_x(1;\,1)R_x(-1;\,1) - R_x^*(1;\,1)R_x^*(-1;\,1) \\ \beta_1 &:= R_x(1;\,1)R_x(-1;\,1) + R_x^*(1;\,1)R_x^*(-1;\,1)\end{aligned}$$

and $\Delta\alpha_1 := \hat{\alpha}_1 - \alpha_1$, $\Delta\beta_1 := \hat{\beta}_1 - \beta_1$. Equation (18) can be equivalently expressed as

$$\hat{f}_e = \frac{P}{4\pi T}\arctan\left(\frac{\alpha_1}{i\beta_1}\cdot\frac{1+\frac{\Delta\alpha_1}{\alpha_1}}{1+\frac{\Delta\beta_1}{\beta_1}}\right). \quad (19)$$

According to [2] and [20], $\Delta\alpha_1$ and $\Delta\beta_1$ are on the order of $o(1/\sqrt{N})$. Considering a Taylor series expansion of the right-hand side of (19) and neglecting the terms of magnitude higher than $o(1/\sqrt{N})$, it follows that

$$\hat{f}_e = \frac{P}{4\pi T} \cdot \left[\arctan\left(\frac{\alpha_1}{i\beta_1}\right) + \frac{\alpha_1}{i\beta_1} \frac{1}{1+\left(\frac{\alpha_1}{i\beta_1}\right)^2} \left(\frac{\Delta\alpha_1}{\alpha_1} - \frac{\Delta\beta_1}{\beta_1}\right) \right]. \quad (20)$$

Simple manipulations of (20) lead to

$$\gamma_{f_e} = \zeta_1^2 \lim_{N\to\infty} N\mathrm{E}\left(\frac{\Delta\alpha_1}{\alpha_1} - \frac{\Delta\beta_1}{\beta_1}\right)^2 = \zeta_1^2 \left(\frac{V_{11}}{\alpha_1^2} + \frac{V_{12}}{\beta_1^2} - \frac{2V_{13}}{\alpha_1\beta_1}\right)$$

where

$$\begin{aligned} \zeta_1 &:= P\tan(4\pi T f_e/P)/[4\pi T(1+\tan^2(4\pi T f_e/P))] \\ V_{11} &:= \lim_{N\to\infty} N\mathrm{E}\{(\Delta\alpha_1)^2\} \\ V_{12} &:= \lim_{N\to\infty} N\mathrm{E}\{(\Delta\beta_1)^2\} \\ V_{13} &:= \lim_{N\to\infty} N\mathrm{E}\{\Delta\alpha_1\Delta\beta_1\}. \end{aligned}$$

Since $\hat{R}_x(k;\tau) = R_x(k;\tau) + o(1/\sqrt{N})$, the previous terms can be easily computed as

$$\begin{aligned} V_{11} &= 2\,\mathrm{re}\left\{\mathbf{R}^T(1)\tilde{\mathbf{\Gamma}}\mathbf{R}(1) - \mathbf{R}^T(1)\mathbf{\Gamma}\mathbf{R}^*(1)\right\} \\ V_{12} &= 2\,\mathrm{re}\left\{\mathbf{R}^T(1)\tilde{\mathbf{\Gamma}}\mathbf{R}(1) + \mathbf{R}^T(1)\mathbf{\Gamma}\mathbf{R}^*(1)\right\} \\ V_{13} &= 2i\,\mathrm{im}\left\{\mathbf{R}^T(1)\tilde{\mathbf{\Gamma}}\mathbf{R}(1)\right\} \end{aligned}$$

where $\mathbf{R}(1) := [R_x(-1;1)\ R_x(1;1)]^T$. According to (7), one can also check that

$$\begin{aligned} \alpha_1 &= 2i\,\frac{\sigma_w^4}{P^2}\sin(4\pi f_e T/P)G^2(1;1) \\ \beta_1 &= 2\,\frac{\sigma_w^4}{P^2}\cos(4\pi f_e T/P)G^2(1;1) \end{aligned}$$

which enables us to conclude the derivation of γ_{f_e} after some simple algebra manipulations of (7).

The derivation of the asymptotic performance of $\hat{\epsilon}$ is more complicated because (10) depends on the estimate of f_e when τ is not equal to 0. Similarly to the derivation presented in (18) and (19), we obtain

$$\hat{\epsilon} = -\frac{1}{2\pi}\arctan\left(\frac{\alpha_2}{i\beta_2}\cdot\frac{1+\frac{\Delta\alpha_2}{\alpha_2}}{1+\frac{\Delta\beta_2}{\beta_2}}\right)$$

where

$$\begin{aligned} \alpha_2 &= R_x(1;1)e^{-2i\pi(f_eT+1/2)/P} - R_x^*(1;1)e^{2i\pi(f_eT+1/2)/P} \\ \beta_2 &= R_x(1;1)e^{-2i\pi(f_eT+1/2)/P} + R_x^*(1;1)e^{2i\pi(f_eT+1/2)/P} \\ \Delta\alpha_2 &= \hat{R}_x(1;1)e^{-2i\pi(\hat{f}_eT+1/2)/P} - \hat{R}_x^*(1;1)e^{2i\pi(\hat{f}_eT+1/2)/P} \\ &\quad - R_x(1;1)e^{-2i\pi(f_eT+1/2)/P} + R_x^*(1;1)e^{2i\pi(f_eT+1/2)/P} \\ \Delta\beta_2 &= \hat{R}_x(1;1)e^{-2i\pi(\hat{f}_eT+1/2)/P} + \hat{R}_x^*(1;1)e^{2i\pi(\hat{f}_eT+1/2)/P} \\ &\quad - R_x(1;1)e^{-2i\pi(f_eT+1/2)/P} - R_x^*(1;1)e^{2i\pi(f_eT+1/2)/P}. \end{aligned}$$

Then, the asymptotic variance of $\hat{\epsilon}$ can be expressed as

$$\gamma_\epsilon = \zeta_2^2 \lim_{N\to\infty} N\mathrm{E}\left(\frac{\Delta\alpha_2}{\alpha_2} - \frac{\Delta\beta_2}{\beta_2}\right)^2 = \zeta_2^2\left(\frac{V_{21}}{\alpha_2^2} + \frac{V_{22}}{\beta_2^2} - \frac{2V_{23}}{\alpha_2\beta_2}\right) \quad (21)$$

where

$$\begin{aligned} \zeta_2 &:= \tan(2\pi\epsilon)/[2\pi(1+\tan^2(2\pi\epsilon))] \\ V_{21} &:= \lim_{N\to\infty} N\mathrm{E}\{(\Delta\alpha_2)^2\} \\ V_{22} &:= \lim_{N\to\infty} N\mathrm{E}\{(\Delta\beta_2)^2\} \\ V_{23} &:= \lim_{N\to\infty} N\mathrm{E}\{\Delta\alpha_2\Delta\beta_2\}. \end{aligned}$$

The term V_{21} can be rewritten as

$$V_{21} = \lim_{N\to\infty} N\mathrm{E} \cdot \left\{ \left[e^{-(2i\pi(\hat{f}_eT+1/2)/P)}\delta_1 - e^{2i\pi(\hat{f}_eT+1/2)/P}\delta_1^* + e^{-i(\pi/P)}R_x(1;1)\delta_2 - e^{i(\pi/P)}R_x^*(1;1)\delta_2^* \right]^2 \right\}$$

where

$$\delta_1 = \hat{R}_x(1;1) - R_x(1;1)$$

and

$$\delta_2 = e^{-2i\pi\hat{f}_eT/P} - e^{-2i\pi f_eT/P}.$$

A first-order Taylor series expansion implies further that

$$\delta_2 = -\frac{2i\pi T}{P}e^{-2i\pi f_eT/P}(\hat{f}_e - f_e) = -\frac{2i\pi T}{P}e^{-2i\pi f_eT/P}\zeta_1\left(\frac{\Delta\alpha_1}{\alpha_1} - \frac{\Delta\beta_1}{\beta_1}\right).$$

After defining the intermediary variables

$$\begin{aligned} \lambda_1 &:= \frac{2i\pi T}{P}\zeta_1\lambda e^{2i\pi f_eT/P} \\ \lambda_2 &:= -\frac{2i\pi T}{P}\zeta_1\lambda e^{-2i\pi f_eT/P} \end{aligned}$$

and

$$\lambda := \left(\frac{1}{\alpha_1} - \frac{1}{\beta_1}\right)\left[R_x(1;1)\tilde{\mathbf{\Gamma}}_{1,1}^{(1,-1)} + R_x(-1;1)\tilde{\mathbf{\Gamma}}_{1,1}^{(1,1)}\right] - \left(\frac{1}{\alpha_1} + \frac{1}{\beta_1}\right)\left[R_x^*(1;1)\mathbf{\Gamma}_{1,1}^{(1,-1)} + R_x^*(-1;1)\mathbf{\Gamma}_{1,1}^{(1,1)}\right]$$

it follows that

$$\begin{aligned} V_{21} &= 2\,\mathrm{re}\left(e^{-4i\pi(f_eT/P+1/2P)}\tilde{\mathbf{\Gamma}}_{1,1}^{(1,1)}\right) - 2\mathbf{\Gamma}_{1,1}^{(1,1)} + 4\,\mathrm{re}\left(e^{-2i\pi(f_eT/P+1/P)}\lambda_2 R_x(1;1)\right) \\ &\quad - 4\,\mathrm{re}\left(e^{-2i\pi f_eT/P}\lambda_1 R_x^*(1;1)\right) - 4\,\mathrm{im}^2\left(\frac{2i\pi T}{P}e^{-2i\pi(f_eT/P+1/2P)}R_x(1;1)\right)\gamma_{f_e}. \end{aligned} \quad (22)$$

The expressions of V_{22} and V_{23}, as well as the remaining parts of the other propositions, can be derived using similar arguments. Moreover, according to (7), we obtain that

$$\alpha_2 = -2i\,\frac{\sigma_w^2}{P}\,\sin(2\pi\epsilon)G(1;\,1) \tag{23}$$

and

$$\beta_2 = 2\,\frac{\sigma_w^2}{P}\,\cos(2\pi\epsilon)G(1;\,1). \tag{24}$$

Finally, plugging (7), (23), and (24) back into (21) and (22) concludes the proof.

REFERENCES

[1] A. Chevreuil, E. Serpedin, P. Loubaton, and G. B. Giannakis, "Blind channel identification and equalization using periodic modulation precoders: Performance analysis," *IEEE Trans. Signal Processing*, vol. 48, pp. 1570–1586, June 2000.

[2] P. Ciblat, P. Loubaton, E. Serpedin, and G. B. Giannakis, "Asymptotic analysis of blind cyclic correlation based symbol-rate estimators," *IEEE Trans. Inform. Theory*, to be published.

[3] ——, "Performance analysis of blind carrier frequency offset estimators for noncircular transmissions through frequency-selective channels," *IEEE Trans. Signal Processing*, vol. 50, pp. 130–140, Jan. 2002.

[4] A. V. Dandawate and G. B. Giannakis, "Nonparametric polyspectral estimators for kth-order (almost) cyclostationary processes," *IEEE Trans. Inform. Theory*, vol. 40, pp. 67–84, Jan. 1994.

[5] G. B. Giannakis, "Cyclostationary signal analysis," in *Digital Signal Processing Handbook*, V. K. Madisetti and D. Williams, Eds. Boca Raton, FL: CRC, 1998.

[6] M. Ghogho, A. Swami, and T. Durrani, "On blind carrier recovery in time-selective fading channels," in *Proc. 33rd Asilomar Conf. Signals, Syst., Comput.*, vol. 1, 1999, pp. 243–247.

[7] F. Gini and G. B. Giannakis, "Frequency offset and symbol timing recovery in flat-fading channels: A cyclostationary approach," *IEEE Trans. Commun.*, vol. 46, pp. 400–411, Mar. 1998.

[8] L. Izzo and A. Napolitano, "Higher-order cyclostationary properties of sampled time-series," *Signal Process.*, vol. 54, no. 3, pp. 303–307, Nov. 1996.

[9] U. Mengali and A. N. D' Andrea, *Synchronization Techniques for Digital Receivers*. New York: Plenum, 1997.

[10] A. Napolitano, "Cyclic higher-order statistics: Input/output relations for discrete- and continuous-time MIMO linear almost-periodically time-variant systems," *Signal Process.*, vol. 42, no. 2, pp. 147–166, Mar. 1995.

[11] A. V. Oppenheim and R. W. Schafer, *Discrete-Time Signal Processing*. Englewood Cliffs, NJ: Prentice-Hall, 1989.

[12] J. G. Proakis, *Digital Communications*, 3rd ed. New York: McGraw-Hill, 1995.

[13] T. S. Rappaport, *Wireless Communications: Principles and Practice*. Englewood Cliffs, NJ: Prentice-Hall, 1996.

[14] K. E. Scott and E. B. Olasz, "Simultaneous clock phase and frequency offset estimation," *IEEE Trans. Commun.*, vol. 43, pp. 2263–2270, July 1995.

[15] C. M. Spooner, "Chapter 2: Higher-order statistics for nonlinear processing of cyclostationary signals," in *Cyclostationary in Communications and Signal Processing*, W. A. Gardner, Ed. New York: IEEE Press, 1993.

[16] C. M. Spooner and W. A. Gardner, "The cumulant theory of cyclostationary time-series, Part II: Development and applications," *IEEE Trans. Signal Processing*, vol. 42, pp. 3409–3429, Dec. 1994.

[17] L. Tong, G. Xu, B. Hassibi, and T. Kailath, "Blind channel identification based on second-order statistics: A frequency-domain approach," *IEEE Trans. Signal Processing*, vol. 41, pp. 329–334, Jan. 1995.

[18] L. Tong, "Joint blind signal detection and carrier recovery over fading channel," in *Proc. ICASSP*, vol. V, Detroit, MI, 1995, pp. 1205–1208.

[19] G. Vazquez and J. Riba, "Non-data aided digital synchronization," in *Signal Processing Advances in Wireless and Mobile Communications*, G. B. Giannakis, Y. Hua, P. Stoica, and L. Tong, Eds. Englewood Cliffs, NJ: Prentice-Hall, 2001, vol. 1, ch. 9, pp. 357–402.

[20] P. Ciblat, P. Loubaton, E. Serpedin, and G. B. Giannakis, "Asymptotic analysis of blind cyclic correlation based symbol-rate estimators," in *Proc. EUSIPCO*, vol. 3, 2000, pp. 1581–1584. [Online]. Available: http://ee.tamu.edu/~serpedin.

Yan Wang received the B.S. degree from the Department of Electronics, Peking University, Beijing, China, in 1996 and the M.Sc. degree from the School of Telecommunications Engineering, Beijing University of Posts and Telecommunications (BUPT), in 1999.

From 1999 to 2000, he was a member of BUPT-Nortel R&D Center, Beijing. Since 2000, he has been a Research Assistant with the Department of Electrical Engineering, Texas A&M University, College Station. His research interests are in the area of statistical signal processing and its applications in wireless communication systems.

Philippe Ciblat was born in Paris, France, in 1973. He received the Engineer degree from Ecole Nationale Supérieure des Télécommunications (ENST), Paris, the M.Sc. in signal processing from University of Paris-Sud, Orsay, France, in 1996, and the Ph.D. degree from the University of Marne-la-Vallée, Noisy le Grand, France, in July 2000.

From October 2000 to June 2001, he was a Postdoctoral Researcher with the Communications and Remote Sensing Department, Université Catholique de Louvain, Louvain-la-Neuve, Belgium. He is currently an Associate Professor with the Department of Communications and Electronics, ENST. His research areas include statistical and digital signal processing, especially blind equalization and synchronization.

Erchin Serpedin received (with highest distinction) the Diploma of electrical engineering form the Polytechnic Institute of Bucharest, Bucharest, Romania, in 1991. He received the specialization degree in signal processing and transmission of information from Ecole Superiéure D'Electricité, Paris, France, in 1992, the M.Sc. degree from Georgia Institute of Technology, Atlanta, in 1992, and the Ph.D. degree from the University of Virginia, Charlottesville, in December 1998.

From 1993 to 1995, he was an instructor with the Polytechnic Institute of Bucharest, and between January and June 1999, he was a Lecturer with the University of Virginia. In July 1999, he joined the Wireless Communication Laboratory, Texas A&M University, College Station, as an Assistant Professor. His research interests lie in the areas of statistical signal processing and wireless communications.

Dr. Serpedin received the NSF Career Award in 2001.

Philippe Loubaton (M'91) was born in 1958 in Villers Semeuse, France. He received the M.Sc. and Ph.D. degrees from Ecole Nationale Supérieure des Télécommunications (ENST), Paris, France, in 1981 and 1988, respectively.

From 1982 to 1986, he was a Member of Technical Staff of Thomson CSF/RGS, where he worked in digital communications. From 1986 to 1988, he was with the Institut National des Télécommunications as an Assistant Professor of electrical engineering. In 1988, he joined ENST, where he worked in the Signal Processing Department. Since 1995, he has been Professor of electrical engineering at the University of Marne-la-Vallée, Noisy le Grand, France. His present research interests are in statistical signal processing and linear system theory, including connections with interpolation theory for matrix-valued holomorphic functions and system identification.

Dr. Loubaton is a member of the board of the GDR/PRC ISIS (the CNRS research group on signal and image processing). He is in charge of the working group on blind identification.